

HOSTED BY



Contents lists available at ScienceDirect

Journal of King Saud University – Science

journal homepage: www.sciencedirect.com

Original article

Spinach protein-capped silver nanoparticles with low hemolytic activity inhibit methicillin-resistant *Staphylococcus aureus* biofilm formation as a new therapeutic approach



Abeer A. Al-Masri

Department of Physiology, College of Medicine, King Saud University, Riyadh 11451, Saudi Arabia

ARTICLE INFO

Article history:

Received 3 July 2023

Revised 12 August 2023

Accepted 12 September 2023

Available online 16 September 2023

Keywords:

Cardiovascular MRSA biofilm

Spinach protein

Silver nanoparticles

Biocompatible

ABSTRACT

Background: The methicillin-resistant *Staphylococcus aureus* (MRSA) was designated as a high-priority pathogen by the World Health Organization. Cardiovascular and thoracic surgery complications frequently involve MRSA infection. Treatment of newly emerging resistant *S. aureus* strains is clinically challenging due to the natural tendency of MRSA survival through biofilm formation. The failure of traditional antibiotic therapy necessitates development of next-generation therapeutic molecules.

Objectives: Silver nanoparticles were investigated to treat MRSA in order to overcome the challenges of antibiotic therapy.

Methods: Spinach protein functionalized silver nanoparticles (SPAgNPs) were synthesized by reducing with sodium borohydride. The resazurin microtiter assay was used to determine the minimum inhibitory concentration (MIC) of SPAgNPs against MRSA. The antibiofilm activity was investigated using a crystal violet assay at sub-MIC levels and validated using scanning electron microscopy. To demonstrate the mechanism of action of SPAgNPs, the virulence factors involved in MRSA biofilm formation were examined. SEM was used to evaluate the hemocompatibility of human red blood cells.

Results and conclusion: The synthesized SPAgNPs showed characteristic yellow colour with surface Plasmon resonance maximum at 418 nm. Powder X-ray diffraction and transmission electron microscopy analysis confirmed that the particles are crystalline with a size range from 14 to 40 nm. SPAgNPs have antibacterial activity at a minimum inhibitory concentration (MIC) of 1.25 mM, killing MRSA via disrupting membrane integrity and producing excess reactive oxygen species. Strikingly, SPAgNPs inhibit MRSA biofilm formation at sub-MIC (0.625 mM). Scanning electron microscopy study reveals that SPAgNPs trigger biofilm inhibition without causing cell damage. Hence the NPs are very effective in preventing pathogens from triggering stress responses. SPAgNPs suppress exopolysaccharide production, cell surface hydrophobicity, and staphyloxanthin biosynthesis. Testing SPAgNPs against human red blood cells reveals that NPs do not harm human cells, suggesting that the SPAgNPs are biocompatible. The findings show that SPAgNPs could be explored as next-generation materials for treating MDR pathogenic infection linked with biofilms.

© 2023 The Author(s). Published by Elsevier B.V. on behalf of King Saud University. This is an open access article under the CC BY-NC-ND license (<http://creativecommons.org/licenses/by-nc-nd/4.0/>).

E-mail address: aemasri@ksu.edu.sa

Peer review under responsibility of King Saud University.



Production and hosting by Elsevier

1. Introduction

The alarming identification rate of antibiotic-resistant bacteria in hospital environments threatens antimicrobial therapy (Avershina et al., 2021). Methicillin-resistant *Staphylococcus aureus* (MRSA) is one of the most prevalent types of infection contracted in hospitals (Álvarez et al., 2019). MRSA has been identified on hospital surfaces and is known to prolong survival in dry environments (Bhardwaj et al., 2020). Surgical sites and prosthetics used are highly vulnerable to MRSA infection. The infections caused by the prosthetic valves used in cardiovascular surgeries are called prosthetic valve endocarditis (Galar et al., 2019). MRSA has been

<https://doi.org/10.1016/j.jksus.2023.102906>

1018-3647/© 2023 The Author(s). Published by Elsevier B.V. on behalf of King Saud University.

This is an open access article under the CC BY-NC-ND license (<http://creativecommons.org/licenses/by-nc-nd/4.0/>).

found as one of the most common pathogens causing post-viral bacterial pneumonia, particularly in patients infected with the influenza type A virus (Ganji et al., 2019). According to the Centres for Disease Control and Prevention (CDC) - United States, around 119,000 people are infected with MRSA yearly, resulting in nearly 20,000 deaths (Kavanagh, 2019). MRSA has been designated as a high-priority pathogen by the World Health Organisation and has called for the development of new medications to combat rising MRSA infections (Adekoya et al., 2021).

Bacteria adopt multiple mechanisms to develop resistance, and one of the widely studied resistant mechanisms is biofilm formation (de Brito et al., 2022). Bacteria produce an extracellular matrix called biofilm, an important virulent factor that protects the pathogens from external agents like antibiotics, where the bacteria reside inside, colonize and spread the infections (Limoli et al., 2015). Thus, alternate therapy regimens targeting the pathogen's virulence must be considered to overcome conventional antibiotics' limitations for treating bacterial infections. Researchers are searching for newer therapeutic modalities to combat drug-resistant bacteria. One of the promising findings in the last two decades was nanoparticles (NPs) made with noble metals like silver, gold, and platinum (Megarajan et al., 2022; Begum et al., 2021; Ayaz Ahmed et al., 2018). The nanodimension adds unique functionality to the metals, but maintaining the materials in nano size is challenging. Hence, capping agents derived chemically and biologically were used to protect the NPs from agglomeration (Ayaz Ahmed et al., 2014; Saravanan et al., 2018; Ameen et al., 2019). Among NPs, silver NPs (AgNPs) were more popular owing to their excellent optoelectronic properties and antibacterial activity against Gram-positive and Gram-negative bacteria (Alarjani et al., 2022; Seralathan et al., 2014). AgNPs elucidate toxicity against microbes by disturbing the cell membrane, altering membrane permeability, and producing excess reactive oxygen species (ROS) (Subramaniyan et al., 2021). Recent studies showed that AgNPs have side effects like toxicity to aquatic animals and mammalian cells (Devi et al., 2015; Cazenave et al., 2019; Milić et al., 2015). Therefore, using AgNPs as an antibacterial has been hampered, but the beneficial nature of NPs demands coordinated research efforts to find safer and non-toxic. To overcome toxicity, greener capping agents such as plant extract, microbial extract, and isolated biomolecules like carbohydrates, proteins, secondary metabolites, and so forth are explored (Venkatakrishnan et al., 2014; Alsamhary et al., 2020; Ameen et al., 2018). Nutraceutical Kaempferitrin functionalized metal NPs are non-toxic when tested in zebrafish animal model but exerts antibacterial activity and cure infected zebrafish by reducing bacterial bioburden (Shamprasad et al., 2022). Pectin-capped platinum NPs showed low toxicity against zebrafish but disrupted the integrity of bacterial membranes and produced excess ROS to kill bacteria (Ahmed et al., 2016). Copper sulfide NPs stabilized with biomimetic lipid showed good hemocompatibility with human red blood cells but damaged bacterial membranes and exhibited antibacterial activity against *Escherichia coli*, *Aeromonas hydrophila*, *Staphylococcus aureus*, and *Bacillus subtilis* (Khan Behlol and Anbazhagan, 2017). These studies suggest that the NPs functionalized with biomolecules/biomimetic molecules offer non-toxic materials with potential therapeutic values. In this work, spinach protein functionalized AgNPs (SPAgNPs) were synthesized and demonstrated their antibacterial and antibiofilm activity against methicillin-resistant *S. aureus* (MRSA). Proteins in the plant leaf mediate photosynthesis through an electron transfer reaction (Guan et al., 2018). Ahmed et al., reported that the spinach protein reduces the Ag^+ to Ag^0 in sunlight (Ahmed et al., 2015). Herein, we reported a modified rapid reduction procedure to prepare the SPAgNPs within 1 min and reported the antibiofilm potential of SPAgNPs against MRSA. The mechanism of antibacterial and antibiofilm action was studied and discussed.

2. Material and methods

2.1. Preparation of spinach protein-capped silver nanoparticles

Spinach protein required for the NPs synthesis was isolated from the spinach leaves as described previously (Ahmed et al., 2015). Typically, 100 g fresh spinach was homogenized in 100 mL PBS buffer, pH 8.0 and the aqueous extract was collected by filtration. The lipophilic pigments and other organic soluble molecules are removed by washing the extract with ice-cold acetone. The resultant aqueous fraction was precipitated by adding 50 % ammonium sulphate. The precipitated was washed thrice with 50 mL of ethanol and assayed for phytochemicals using the reported procedure (Dharshini et al., 2023). The qualitative phytochemical analysis answered positively for the presence of proteins. Hence, the protein concentration was quantified by Lowry assay using bovine serum albumin as standard.

Spinach protein-capped silver nanoparticles were prepared using the reported procedure with slight modification (Ahmed et al., 2015). Briefly, 1 mg/mL spinach protein was mixed with 10 mM $AgNO_3$ and followed by 10 mM sodium borohydride. The colour change to yellow within 1 min confirms the formation of AgNPs. High-resolution transmission electron microscopy (HRTEM; JEOL, Japan) were employed to measure the size, shape, and crystallinity. The powder X-ray diffraction of the SPAgNPs was measured in an XRD-Bruker D8 Advance X-ray diffractometer with monochromatic $Cu K\alpha$ radiation.

2.2. Antibacterial assays

The minimum inhibitory concentration of SPAgNPs against methicillin-resistant *Staphylococcus aureus* (ATCC 33591) was identified by the use of microdilution procedures as with a small modification (Selvaraj et al., 2020). Typically, 50 μ L of 0.1 OD MRSA in LB media was put into 96-well plates containing 10 mM SPAgNPs, and incubated for 12 h at 37 °C. Thermo Scientific Multiscan EX, a microtiter plate reader, measured the optical density at 600 nm in each well. Resazurin (30 μ L, 0.01% wt/v) was added and incubated to test for cell viability after 12 h (Coban, 2012). Dead to viable cells are indicated by a color change from blue to pink, which is labeled as MIC.

To determine the impact of SPAgNPs on the membrane permeability of MRSA, a propidium iodide (PI) uptake experiment was carried out (Crowley et al., 2016). Typically, 0.5 OD MRSA was treated for 2 h at 37 °C with 0.5X, 1X, and 2X MIC of SPAgNPs. After treatment, the cells were centrifuged and the pellet was exposed to 0.5 M PI. Using the JASCO spectrofluorometer FP-8200, the PI fluorescence emission was measured at 600 nm (excitation at 543 nm). The fluorescence from untreated cells (F_0), and the cells treated with cetyl trimethyl ammonium (F_{100}) serves as negative and positive control, respectively. F_{obs} are the fluorescence from cells treated with SPAgNPs. The membrane permeability was obtained from the equation (2).

$$\% \text{ membrane permeability} = [(F_{obs} - F_0)/(F_{100} - F_0)] \times 100 \quad (1)$$

Dichlorofluorescein diacetate (H2DCFDA) assay was employed to determine the production of reactive oxygen species in MRSA (Bezza et al., 2020). Typically, 0.5 OD MRSA was treated with SPAgNPs as described above, then exposed to 0.5 M H2DCFDA and incubated at dark for 30 min. The H2DCFDA diffuse the cell membranes and is deacylated by intracellular esterase to produce weakly fluorescent 2',7' dichlorodihydrofluorescein (H2DCF). While exposed to ROS, H2DCF oxidizes to produce fluorescence from the cells were measured using excitation and emission wavelength of 2',7', dichlorofluorescein (DCF), which will be monitored

with excitation and emission wavelengths of 498 nm and 522 nm, respectively. H_2O_2 serves as a positive control. The percentage ROS production was calculated using equation (1).

2.3. Antibiofilm assays

An overnight grown MRSA culture in LB media diluted to 1% Tryptic Soy Broth (TSB) was added to the 96-well plate. Typically, 10 mM SPAgNPs were serially diluted to find the minimal biofilm inhibitory concentration (MBIC). A 100 μ L aliquot of MRSA was added to the 96-well plate (Bala Subramaniyan et al., 2020) and incubated at 37 °C for 24 h. The medium was carefully removed, cleaned three times in PBS buffer to remove any unattached cells. Then, the cells stained with 0.1% crystal violet (CV) for 20 min. The unbound CV was removed by PBS washing and the stained biofilm was dried at 60 °C. A 30% acetic acid extraction was performed on the bound CV. At 595 nm, the CV extract's absorbance was measured, and the inhibition percentage was calculated.

$$\% \text{ of biofilm inhibition} = \left[\frac{(\text{ControlOD} - \text{TestOD})}{(\text{ControlOD})} \right] \times 100 \quad (2)$$

Microorganisms were cultured in 24-well plates for 24 h at 37 °C in the absence and presence of SPAgNPs to determine the

extracellular polymeric substance (EPS). MRSA produces EPS in TSB media, a crucial constituent of biofilm (Sugimoto et al., 2018). The absorbance of the EPS was extracted by the mixture of sulfuric acid and phenol (5% v/v) was recorded at measured at 490 nm.

The microbial adhesion to hydrocarbon (MATH) in the presence and absence of SPAgNPs was tested to quantify the hydrophobicity of the cell surface (Selvaraj et al., 2020). SPAgNPs were used to treat 0.5 OD of MRSA for 2 h at 37 °C. After treatment, the cells were collected by centrifugation and reconstituted in 1 mL PBS buffer. A phase separation occurs after adding 1 mL of toluene to the PBS mixture and 10 min of vigorous vortexing. After separating the aqueous phase, the absorbance at 600 nm was determined. Equation (3) was used to get the % hydrophobicity.

$$\% \text{ hydrophobicity} = \left[1 - \frac{(\text{OD}_{600\text{nm}} \text{ after vortexing})}{(\text{OD}_{600\text{nm}} \text{ before vortexing})} \right] \times 100 \quad (3)$$

2.4. Staphyloxanthin assay

MRSA was cultured overnight in TSB broth with and without SPAgNPs. After 24 h incubation at 37 °C, the pellet was obtained by centrifuging the culture at 10,000 rpm for 10 min at 4 °C with an Eppendorf 5424R refrigerated centrifuge, followed by three

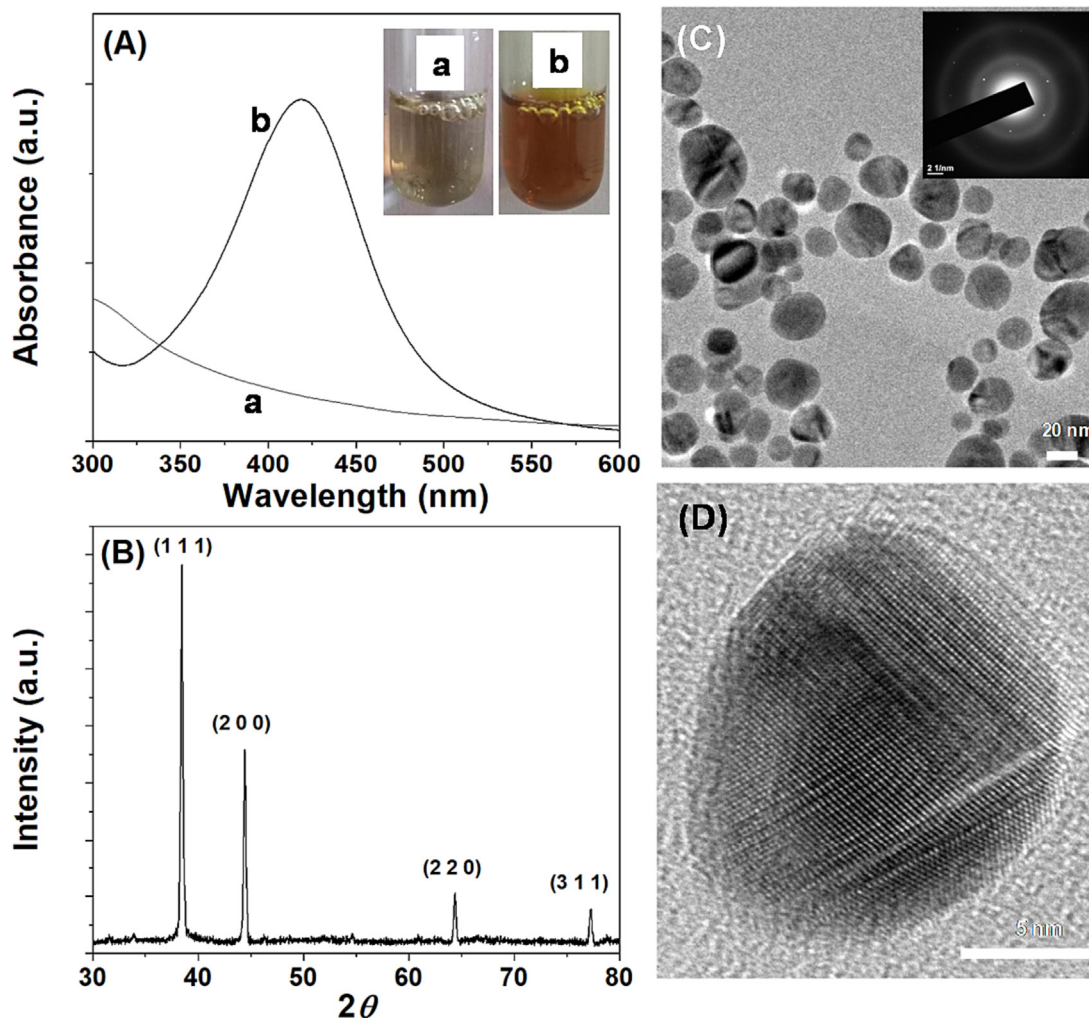


Fig. 1. Characterization of SPAgNPs. (A) UV-Visible spectrum, inset corresponds to the photograph of the solution (a) spinach protein and (b) SPAgNPs. (B) Power XRD shows the various facets of AgNPs, (C) TEM images show the spherical NPs, the inset corresponds to the SAED pattern, and (D) HRTEM shows the lattice fringes in the NPs, confirming crystalline.

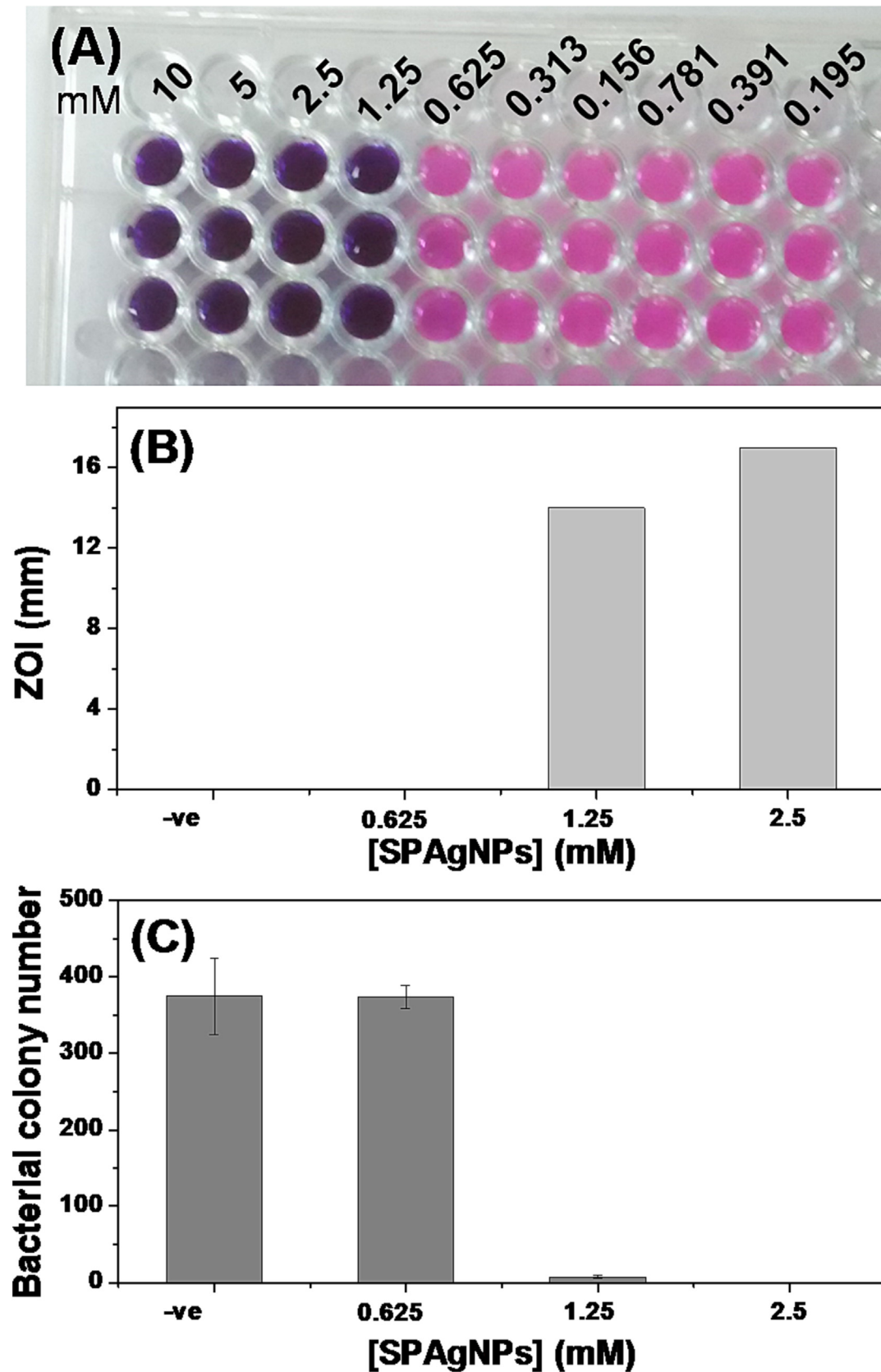


Fig. 2. Antibacterial activity. (A) MIC determination using REMA. Blue colour and pink indicate non-respiratory and live cells, respectively. 10 mM SPAgNPs was added to the first well and serially diluted. Experiments were done in triplicate. (B) Zone of inhibition assay. NPs were added to the well, and the zone formed around the well was measured after 12 h (C) Colony count assay. The cells were treated with NPs, plated on an LB-agar plate, and counted the colonies formed after 12 h. All experiments are carried out in triplicate, and the average values are given as mean \pm SD.

PBS washes. The pellet's yellow colour proves that staphyloxanthin is present.

2.5. Hydrogen peroxide (H₂O₂) sensitivity assay

The sensitivity of MRSA to H₂O₂ in cells treated with SPAgNPs was investigated by (Brioukhanov and Netrusov, 2004).

2.6. Biocompatibility assay

After informed consent was acquired, the trained doctor drew about 5 mL of healthy volunteers' blood and placed it in an anticoagulant solution. The RBC was isolated by centrifuging it at 1500 rpm and resuspended in 10 mL PBS buffer, and used freshly for the study. Typically, 100 μL of 1.25 mM SPAgNPs was exposed to 100 μL RBC and incubated at 37 °C for 2 h. After treatment, the cells were analyzed by TESCAN scanning electron microscope.

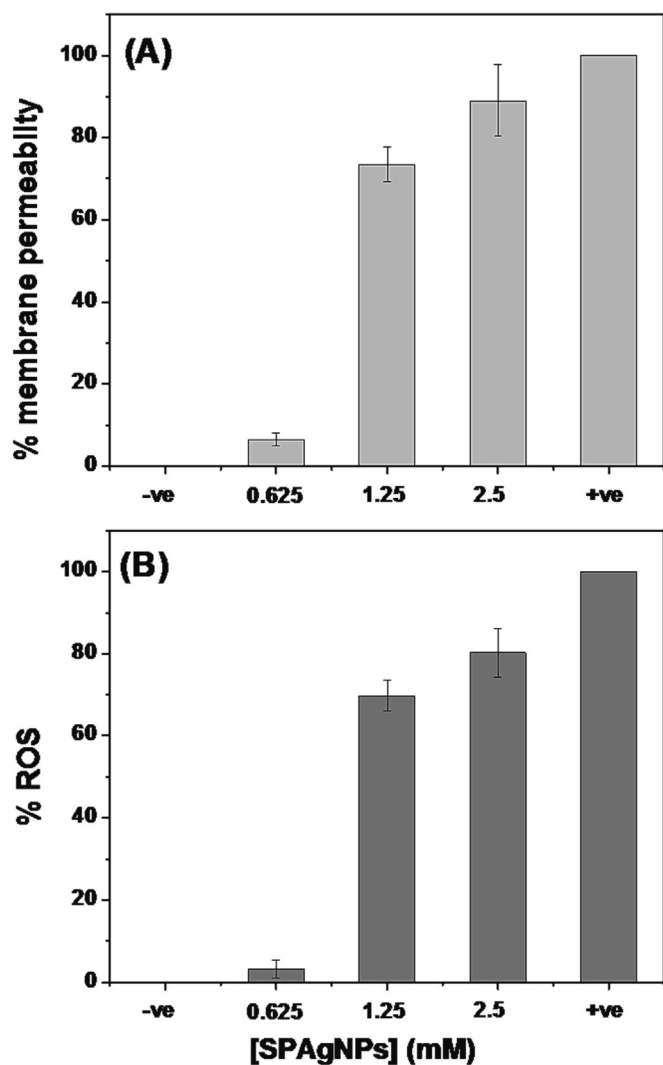


Fig. 3. (A) Membrane integrity assay. -ve control - Untreated cells; +ve control - cells treated with CTAB. (B) ROS assay. -ve control - Untreated cells; +ve control - cells treated with H₂O₂.

3. Results

3.1. Synthesis and characterization of spinach protein-capped AgNPs

Reducing silver ions in the presence of spinach protein produces a yellow colour AgNPs solution in less than one minute, which shows absorption spectra with a maximum at 418 nm (Fig. 1A). SPAgNPs have a zeta potential of -19.2 mV, which is equivalent

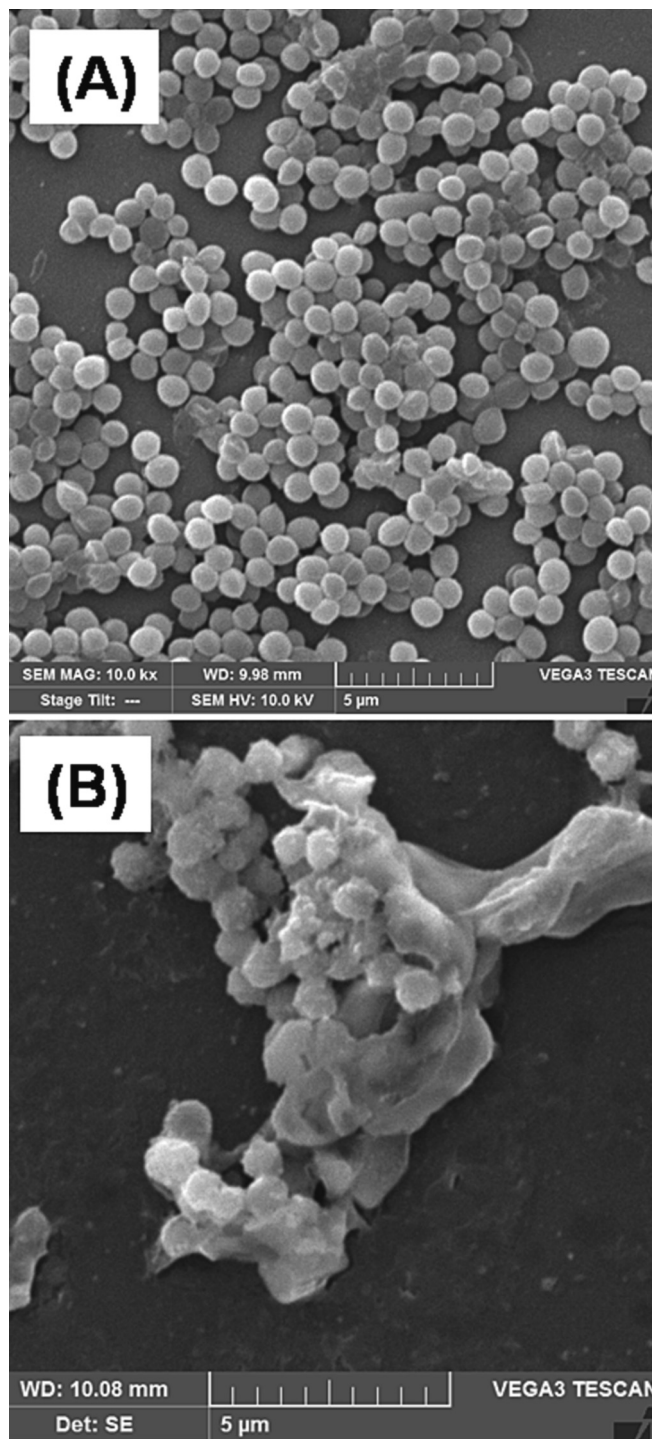


Fig. 4. SEM image of MRSA (A) untreated and (B) treated with 1X MIC of SPAgNPs. Due to membrane damage, the treated cells tend to agglomerate and appear as clusters.

to values reported in the literature for stable AgNPs (Ahmed et al., 2015). Powder X-ray diffraction of SPAgNPs showed four strong Bragg reflections at 38.47° , 44.44° , 64.37° and 77.25° . The interplanar spacing ($d_{\text{calculated}}$) values are 2.822, 1.996, 1.629 and 1.261 Å and matched with the standard powder diffraction card of silver metal (JCPDS 04–0783). The average crystalline size of synthesized SPAgNPs calculated from XRD data using the Debye-Scherrer formula is 38 nm. The morphology and size examined by TEM reveal that the SPAgNPs is spherical with a size range from 14 to 40 nm, which is comparable with the size calculated from pXRD. The con-

centric ring pattern with intermittent dots (inset Fig. 1C) in the selected area electron diffraction (SAED) and the lattice fringes observed in the high-resolution TEM (Fig. 1D) suggests that the SPAgNPs are crystalline.

3.2. Effect of SPAgNPs against MRSA

The minimum inhibitory concentration (MIC) of SPAgNPs against MRSA is 1.25 mM (Fig. 2A). The zone of inhibition (ZOI) method is widely accepted to assess an antibacterial agent's efficiency. The diameter of ZOI measures how well the NPs destroy the bacteria under investigation. The increased zone size of the SPAgNPs at higher concentrations, as shown in Fig. 2B, suggests that the killing of these molecules is concentration dependent. A LB-agar plate was used to plate the MRSA after it had been grown in different SPAgNPs concentrations. The colonies formed on the plates were counted after 12 h. Fig. 2C shows that SPAgNPs at 1X MIC considerably slows bacterial growth when compared to the untreated control.

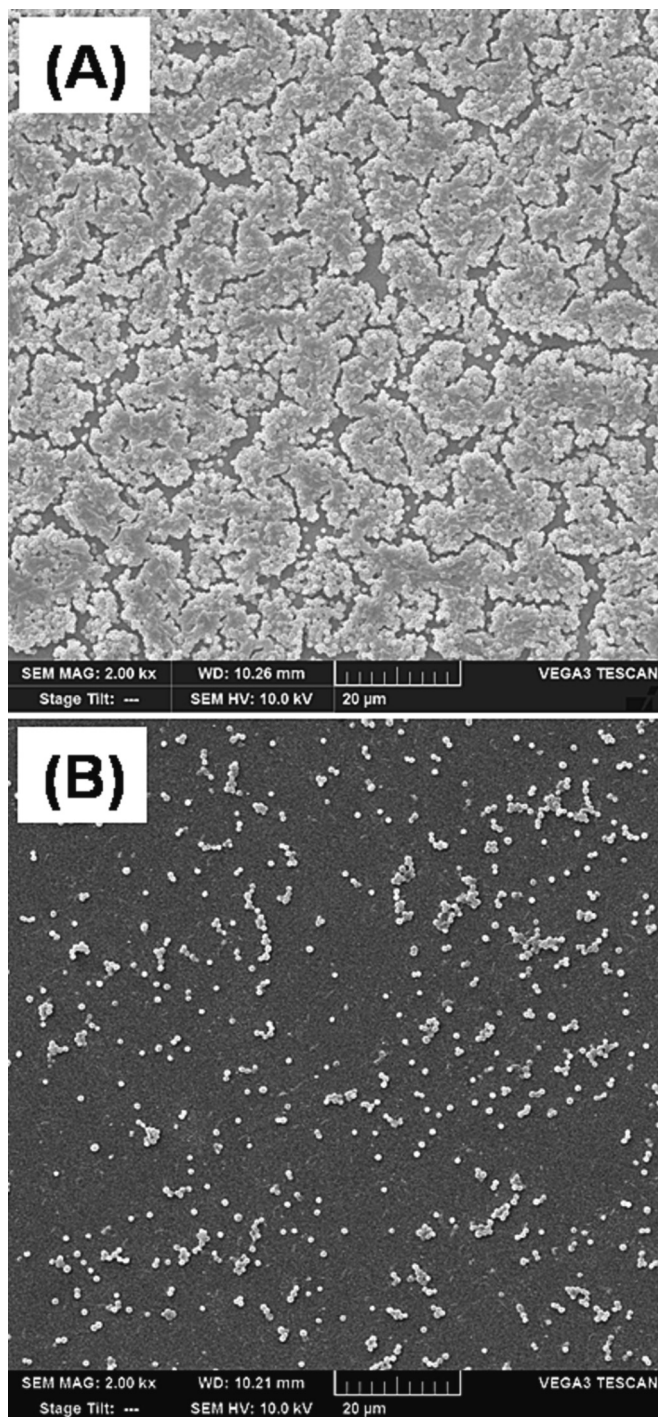


Fig. 5. SEM images of MRSA at 1X MBIC (0.625 mM). It is noted that the morphology of the cells is changed, and membranes are intact.

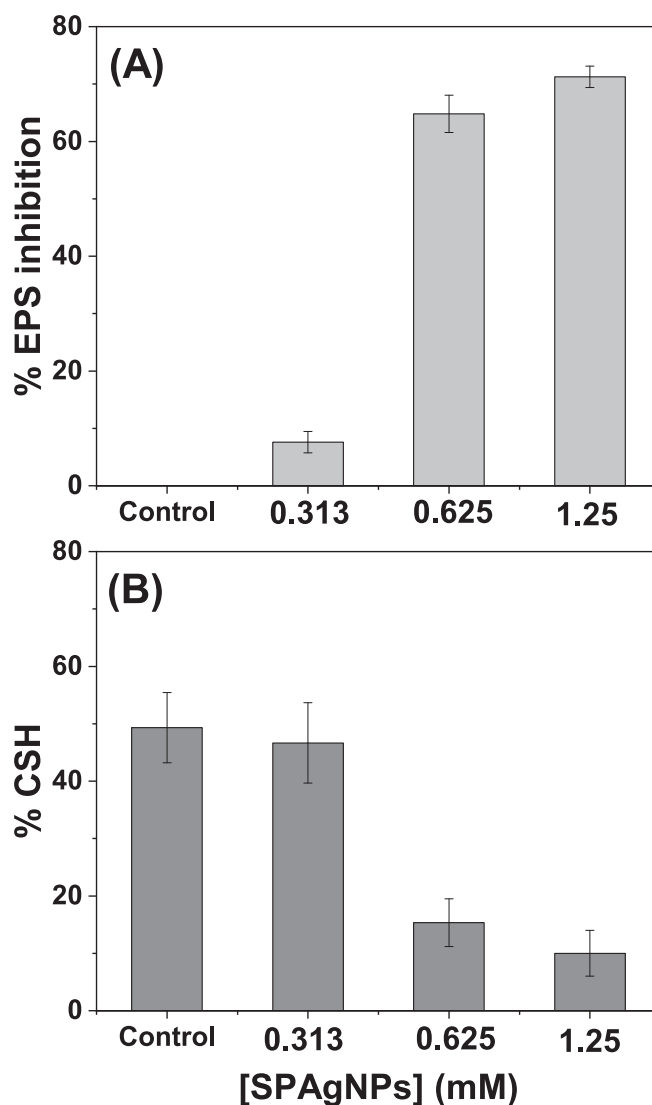


Fig. 6. Effect of SPNPs on (A) EPS production and (B) cell surface hydrophobicity. The experiments are repeated three times, and the average values are given as mean \pm SD.

3.3. Antibacterial mechanism

The influence of SPAgNPs on bacterial membranes was assessed by the fluorescence probe, propidium iodide (PI) (Subramaniyan et al., 2021). The cells treated with SPAgNPs produced strong fluorescence as compared to the untreated control, and about 74 % of the membranes are permeable to SPAgNPs at 1X MIC (Fig. 3A). The observation suggests that the NPs treatment affects the membrane integrity and allows PI to cross the membrane to stain nucleic acid. H2DCFDA assay used to detect ROS production suggests that the cells treated at 1X MIC of SPAgNPs produced excess ROS compared to the untreated cells (Fig. 3B).

To demonstrate how SPAgNPs affects MRSA, SEM images of both untreated and treated cells were analyzed. The untreated cells appear spherical with intact membranes (Fig. 4A) and the cells treated with NPs showed multiple blisters, and bubbles formed on the surface (Fig. 4B), suggesting that the membranes are damaged, and the cellular contents are leaked.

3.4. Biofilm inhibitory activity of SPAgNPs

The minimum biofilm inhibitory concentration (MBIC) of SPAgNPs against MRSA biofilm was deduced by crystal violet assay. The MBIC was 0.625 mM, two-fold lower than the MIC, suggesting that SPAgNPs inhibit biofilm at MBIC without inducing cell death. The SEM pictures taken at the antibiofilm concentration demonstrated that the shape of the cells was unharmed and that the outer membranes were still intact (Fig. 5), suggesting SPAgNPs affect biofilm formation without damaging the cells at MBIC.

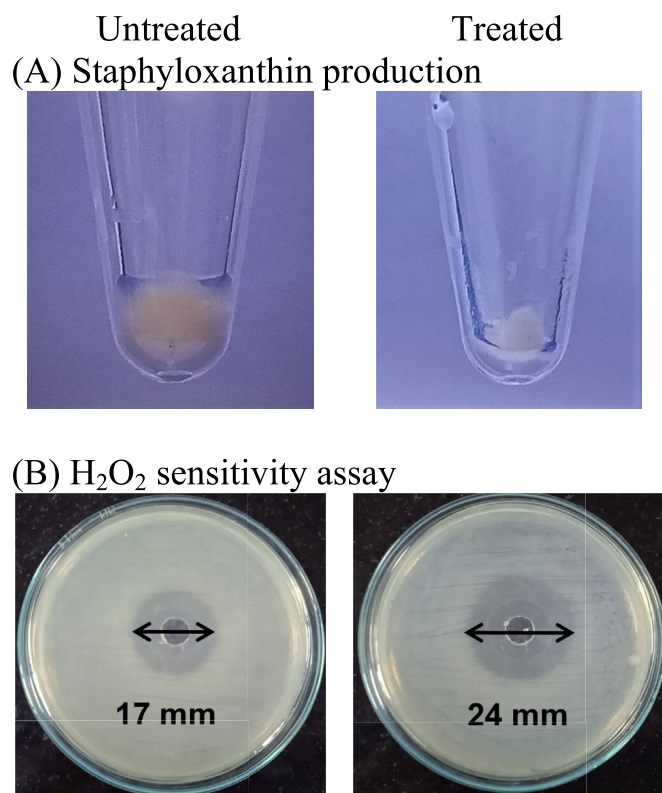


Fig. 7. (A) Staphyloxanthin synthesis in MRSA treated with 0.625 mM SPAgNPs was observed. (B) H₂O₂ sensitivity assay by the well diffusion method. Images on the plate images showed the effect of 0.625 mM SPAgNPs on the sensitivity of MRSA to H₂O₂.

3.5. Biofilm inhibition mechanism of SPAgNPs

The EPS production measured using the phenol sulfuric acid method indicated that 65 % of EPS production was reduced at 1X MBIC of SPAgNPs compared to the untreated control (Fig. 6A). The cell surface hydrophobicity (CSH) measured by MATH assay reveals that SPAgNPs reduce the CSH from 49 % to 15 % at 1X MBIC (Fig. 6B). The findings indicate that SPAgNPs interfere with EPS synthesis, reduce CSH to prevent microbial adhesion, and hinder biofilm formation.

MRSA produces staphyloxanthin, a golden-yellow pigment, to maintain the oxidative stress balance and to elude the host antioxidant defence. Staphyloxanthin, a triterpenoid carotenoid, gives MRSA its golden yellow colour, interestingly; the cells treated with SPAgNPs had a loss of pigmentation, indicating that MRSA had lost its antioxidant defense (Fig. 7A). A further insight into the pathogen antioxidant defense was investigated by peroxide-sensitive assay. Enzymes like catalase and superoxide dismutase play a crucial part in pathogen defense. These enzymes are sensitive to peroxides. MRSA plated on an LB-agar plate in the presence of H₂O₂ showed a zone of clearance of 17 mm. The plate exposed to 0.625 mM SPAgNPs in the presence of H₂O₂ showed a larger zone of clearance (24 mm), suggesting MRSA becomes more sensitive to ROS (Fig. 7B).

3.6. Effect of SPAgNPs on human red blood cells

The RBC exposed to an antibacterial concentration of SPAgNPs (1.25 mM) was imaged in SEM. It is noted from Fig. 8A the

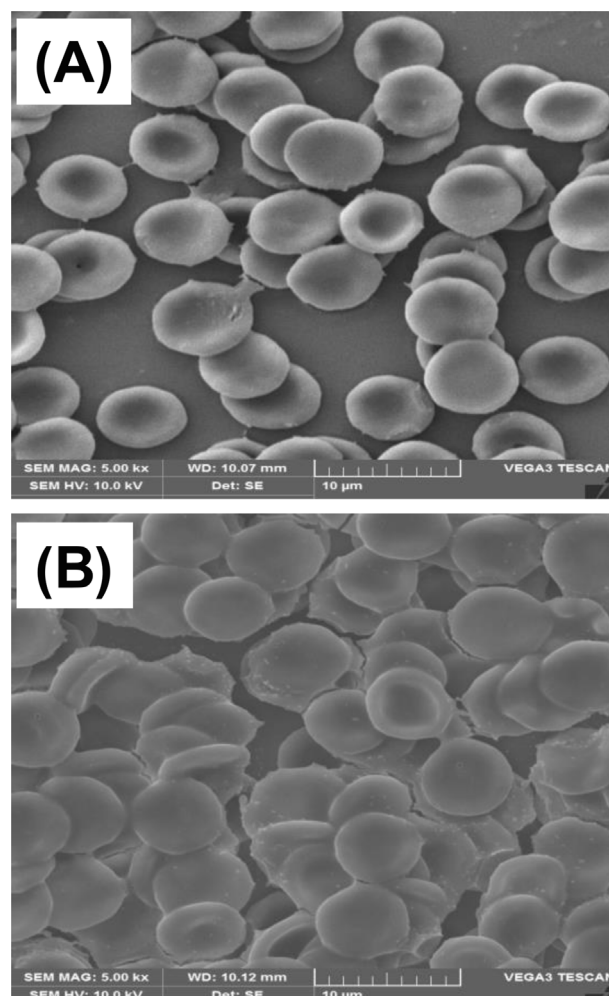


Fig. 8. SEM image of (A) untreated RBC and (B) RBC treated with 1.25 mM SPAgNPs.

untreated RBC and the treated RBC showed similar concave morphology and membranes are intact, indicating that NPs do not induce any changes to the human membranes.

4. Discussion

Spinach leaves contain proteins, which are useful in SPAgNPs synthesis. The yellow colour of SPAgNPs originates from the coherent electron motion, which gives rise to the characteristics of Surface Plasmon Resonance maximum at 418 nm in the UV–Visible spectrum (Fig. 1A). From the powder X-ray diffraction data the size of the NPs was deduced using Debye-Scherrer formula as 38 nm, which is comparable to the size determined by TEM images and the facets are attributed to face centred cubic crystal structure of silver (Ahmed et al., 2015). Most hospital-acquired infections have been linked to MRSA. Being resistant to many medications and becoming resistant to last-resort antibiotics like vancomycin makes it challenging to treat MRSA infections. The MIC determined by REMA is 1.25 mM and the SPAgNPs showed increased ZOI at higher concentration, suggesting that SPAgNPs exhibit concentration dependent activity. This was confirmed by colony formation study, which suggests that SPAgNPs have excellent potential to inhibit MRSA proliferation. SPAgNPs kill the bacteria by promoting excessive ROS production, disrupting the integrity of the membrane, and result in membrane damage, eventually result in bacterial death. The biofilm-forming capacity of MRSA has been recognized as a key virulence factor that protects against the immune system and antibiotics and is considered to be the cause of chronic or persistent infections (Avershina et al., 2021). Thus, inhibiting biofilm formation is an important strategy to combat drug-resistant bacteria infection. SPAgNPs do not disturb the membrane integrity at sub-MIC but prevent the cells from colonization. The prevention of colonization may inhibit cell communication and influence the virulence factors of MRSA. It has been noted that SPAgNPs inhibit EPS synthesis; decrease cell surface hydrophobicity, and inhibit antioxidant enzyme activity to prevent the biofilm formation (Valliammai et al., 2021). The findings revealed that SPAgNPs have good potential to inhibit MRSA biofilm formation. SEM analysis reveals that 1X MIC SPAgNPs affect the MRSA membrane and cell morphology (Fig. 4B). Strikingly, SPAgNPs treated RBC showed intact cells, suggesting that the NPs are non-toxic to mammalian membranes (Fig. 8B). However, further detailed toxicity study in animal models is required to recommend the SPAgNPs for the next testing phase.

5. Conclusion

In summary, SPAgNPs demonstrated a potential impact on the MRSA biofilm without compromising microbial viability. In vitro, tests showed that the SPAgNPs impacted the EPS and CSH production linked to biofilm adherence. Notably, SPAgNPs inhibit the antioxidant defense system of MRSA. SPAgNPs also kill the bacteria by producing excess and affecting the membrane integrity. Testing against human RBC revealed that the antibacterial concentration of SPAgNPs does affect the human cell membranes, suggesting its biocompatibility. The findings show that SPAgNPs have the potential to evolve into an effective therapeutic agent that is contracted from the hospital environment. The results may need to be refined for therapeutic applicability through more studies using mouse models and cell cultures.

Declaration of Competing Interest

The author declares that she has no known competing financial interests or personal relationships that could have appeared to influence the work reported in this paper.

Acknowledgement

The author extends her appreciation to the Deputyship for Research and Innovation, Ministry of Education in Saudi Arabia for funding this research work through the project no. (IFKSUOR3-017-3).

References

- Adekoya, I., Maraj, D., Steiner, L., Yaphe, H., Moja, L., Magrini, N., Cooke, G., Loeb, M., Persaud, N., 2021. Comparison of antibiotics included in national essential medicines lists of 138 countries using the WHO Access, Watch, Reserve (AWaRe) classification: a cross-sectional study. *Lancet Infect. Dis.* 21 (10), 1429–1440. [https://doi.org/10.1016/S1473-3099\(20\)30854-9](https://doi.org/10.1016/S1473-3099(20)30854-9).
- Ahmed, K.B.A., Raman, T., Anbazhagan, V., 2016. Platinum nanoparticles inhibit bacteria proliferation and rescue zebrafish from bacterial infection. *RSC Adv.* 6 (50), 44415–44424. <https://doi.org/10.1039/C6RA03732A>.
- Ahmed, K.B., Senthilnathan, R., Megarajan, S., Anbazhagan, V., 2015. Sunlight mediated synthesis of silver nanoparticles using redox phytoprotein and their application in catalysis and colorimetric mercury sensing. *J. Photochem. Photobiol. B* 151, 39–45. <https://doi.org/10.1016/j.jphotobiol.2015.07.003>.
- Alarjani, K.M., Huessien, D., Rasheed, R.A., Kalaiyarasi, M., 2022. Green synthesis of silver nanoparticles by *Pisum sativum* L. (pea) pod against multidrug resistant foodborne pathogens. *J. King Saud Univ. - Sci.* 34. <https://doi.org/10.1016/j.jksus.2022.101897> 101897.
- Alsamhary, K., Al-Enazi, N., Alshehri, W.A., Ameen, F., 2020. Gold nanoparticles synthesized by flavonoid tricetin as a potential antibacterial nanomedicine to treat respiratory infections causing opportunistic bacterial pathogens. *Microb. Pathog.* 139. <https://doi.org/10.1016/j.micpath.2019.103928> 103928.
- Álvarez, A., Fernández, L., Gutiérrez, D., Iglesias, B., Rodríguez, A., García, P., 2019. Methicillin-resistant *Staphylococcus aureus* in hospitals: latest trends and treatments based on bacteriophages. *J. Clin. Microbiol.* 57 (12), e01006–e01019. <https://doi.org/10.1128/JCM.01006-19>.
- Ameen, F., AlYahya, S.A., Bakhrebah, M.A., Nassar, M.S., Aljuraifani, A., 2018. Flavonoid dihydromyricetin-mediated silver nanoparticles as potential nanomedicine for biomedical treatment of infections caused by opportunistic fungal pathogens. *Res. Chem. Intermed.* 44, 5063–5073. <https://doi.org/10.1007/s11164-018-3409-x>.
- Ameen, F., Srinivasan, P., Selvakumar, T., Kamala-Kannan, S., Al Nadhari, S., Almansob, A., Dawoud, T., Govarthanan, M., 2019. Phytosynthesis of silver nanoparticles using *Mangifera indica* flower extract as bioreductant and their broad-spectrum antibacterial activity. *Bioorg. Chem.* 88. <https://doi.org/10.1016/j.bioorg.2019.102970> 102970.
- Avershina, E., Shapovalova, V., Shipulin, G., 2021. Fighting antibiotic resistance in hospital-acquired infections: current state and emerging technologies in disease prevention, diagnostics and therapy. *Front Microbiol.* 12. <https://doi.org/10.3389/fmicb.2021.707330> 707330.
- Ayaz Ahmed, K.B., Subramanian, S., Sivasubramanian, A., Veerappan, G., Veerappan, A., 2014. Preparation of gold nanoparticles using *Salicornia brachiata* plant extract and evaluation of catalytic and antibacterial activity. *Spectrochim. Acta A Mol. Biomol. Spectrosc.* 130, 54–58. <https://doi.org/10.1016/j.saa.2014.03.070>.
- Ayaz Ahmed, K.B., Raman, T., Veerappan, A., 2018. Jacalin capped platinum nanoparticles confer persistent immunity against multiple *Aeromonas* infection in zebrafish. *Sci. Rep.* 8 (1), 2200. <https://doi.org/10.1038/s41598-018-20627-3>.
- Bala Subramaniyan, S., Senthilnathan, R., Arunachalam, J., Anbazhagan, V., 2020. Revealing the significance of the glycan binding property of butea monosperma seed lectin for enhancing the antibiofilm activity of silver nanoparticles against uropathogenic *Escherichia coli*. *Bioconjug. Chem.* 31 (1), 139–148. <https://doi.org/10.1021/acs.bioconjchem.9b00821>.
- Begum, I., Ameen, F., Soomro, Z., Shamim, S., AlNadhari, S., Almansob, A., Al-Sabri, A., Arif, A., 2021. Facile fabrication of malonic acid capped silver nanoparticles and their antibacterial activity. *J. King Saud Univ. Sci.* 33. <https://doi.org/10.1016/j.jksus.2020.101231> 101231.
- Bezza, F.A., Tichapondwa, S.M., Chirwa, E.M.N., 2020. Fabrication of monodispersed copper oxide nanoparticles with potential application as antimicrobial agents. *Sci. Rep.* 10 (1), 16680. <https://doi.org/10.1038/s41598-020-73497-z>.
- Bhardwaj, N., Khattri, M., Bhardwaj, S.K., Sonne, C., Deep, A., Kim, K.H., 2020. A review on mobile phones as bacterial reservoirs in healthcare environments and potential device decontamination approaches. *Environ. Res.* 186. <https://doi.org/10.1016/j.envres.2020.109569> 109569.
- Brioukhanov, A.L., Netrusov, A.I., 2004. Catalase and superoxide dismutase: distribution, properties, and physiological role in cells of strict anaerobes. *Biochemistry (Mosc.)* 69 (9), 949–962. <https://doi.org/10.1023/b:biry.0000043537.04115.d9>.
- Cazenave, J., Ale, A., Bacchetta, C., Rossi, A.S., 2019. Nanoparticles toxicity in fish models. *Pharm. Des.* 25 (37), 3927–3942. <https://doi.org/10.2174/1381612825666190912165413>.
- Coban, A.Y., 2012. Rapid determination of methicillin resistance among *Staphylococcus aureus* clinical isolates by colorimetric methods. *J. Clin. Microbiol.* 50 (7), 2191–2193. <https://doi.org/10.1128/JCM.00471-12>.

- Crowley, L.C., Scott, A.P., Marfell, B.J., Boughaba, J.A., Chojnowski, G., Waterhouse, N. J., 2016. Measuring cell death by propidium iodide uptake and flow cytometry. *Cold Spring Harb Protoc* 2016 (7). <https://doi.org/10.1101/pdb.prot087163>.
- de Brito, F.A.E., de Freitas, A.P.P., Nascimento, M.S., 2022. Multidrug-resistant biofilms (MDR): main mechanisms of tolerance and resistance in the food supply chain. *Pathogens*. 11 (12), 1416. <https://doi.org/10.3390/pathogens11121416>.
- Devi, G.P., Ahmed, K.B., Varsha, M.K., Shrijha, B.S., Lal, K.K., Anbazhagan, V., Thiagarajan, R., 2015. Sulfidation of silver nanoparticle reduces its toxicity in zebrafish. *Aquat. Toxicol.* 158, 149–156. <https://doi.org/10.1016/j.aquatox.2014.11.007>.
- Dharshini, K.S., Yokesh, T., Mariappan, M., Ameen, F., Amirul Islam, M., Veerappan, A., 2023. Photosynthesis of silver nanoparticles embedded paper for sensing mercury presence in environmental water. *Chemosphere* 329, <https://doi.org/10.1016/j.chemosphere.2023.138610> 138610.
- Galar, A., Weil, A.A., Dudzinski, D.M., Muñoz, P., Siedner, M.J., 2019. Methicillin-resistant *Staphylococcus aureus* prosthetic valve endocarditis: pathophysiology, epidemiology, clinical presentation, diagnosis, and management. *Clin. Microbiol. Rev.* 32 (2), e00041–e118. <https://doi.org/10.1128/CMR.00041-18>.
- Ganji, M., Ruiz, J., Kogler, W., Lung, J., Hernandez, J., Isache, C., 2019. Methicillin-resistant *Staphylococcus aureus* pericarditis causing cardiac tamponade. *IDCases* 18, e00613.
- Guan, X., Chen, S., Voon, C.P., Wong, K.B., Tikkanen, M., Lim, B.L., 2018. FdC1 and leaf-type ferredoxins channel electrons from photosystem I to different downstream electron acceptors. *Front. Plant Sci.* 9, 410. <https://doi.org/10.3389/fpls.2018.00410>.
- Kavanagh, K.T., 2019. Control of MSSA and MRSA in the United States: protocols, policies, risk adjustment and excuses. *Antimicrob. Resist. Infect. Control* 8, 103. <https://doi.org/10.1186/s13756-019-0550-2>.
- Khan Behlol, A.A., Anbazhagan, V., 2017. Synthesis of copper sulfide nanoparticles and evaluation of *in vitro* antibacterial activity and *in vivo* therapeutic effect on bacteria infected zebrafish. *RSC Adv.* 7 (58), 36644–36652. <https://doi.org/10.1039/C7RA05636B>.
- Limoli, D.H., Jones, C.J., Wozniak, D.J., 2015. Bacterial extracellular polysaccharides in biofilm formation and function. *Microbiol. Spectr.* 3 (3). <https://doi.org/10.1128/microbiolspec.MB-0011-2014>.
- Megarajan, S., Ameen, F., Singaravelu, D., Islam, M.A., Veerappan, A., 2022. Synthesis of N-myristoyltaurine stabilized gold and silver nanoparticles: assessment of their catalytic activity, antimicrobial effectiveness and toxicity in zebrafish. *Environ. Res.* 212, (Pt A). <https://doi.org/10.1016/j.envres.2022.113159> 113159.
- Milić, M., Leitinger, G., Pavičić, I., Zebić Avdičević, M., Dobrović, S., Goessler, W., Vinković Vrček, I., 2015. Cellular uptake and toxicity effects of silver nanoparticles in mammalian kidney cells. *J. Appl. Toxicol.* 35 (6), 581–592. <https://doi.org/10.1002/jat.3081>.
- Saravanan, M., Gopinath, V., Chaurasia, M.K., Syed, A., Ameen, F., Purushothaman, N., 2018. Green synthesis of anisotropic zinc oxide nanoparticles with antibacterial and cytofriendly properties. *Microb. Pathog.* 115, 57–63. <https://doi.org/10.1016/j.micpath.2017.12.039>.
- Selvaraj, A., Valliammai, A., Sivasankar, C., Suba, M., Sakthivel, G., Pandian, S.K., 2020. Antibiofilm and antivirulence efficacy of myrtenol enhances the antibiotic susceptibility of *Acinetobacter baumannii*. *Sci. Rep.* 10, 21975. <https://doi.org/10.1038/s41598-020-79128-x>.
- Seralathan, J., Stevenson, P., Subramaniam, S., Raghavan, R., Pemaiah, B., Sivasubramanian, A., Veerappan, A., 2014. Spectroscopy investigation on chemo-catalytic, free radical scavenging and bactericidal properties of biogenic silver nanoparticles synthesized using *Salicornia brachiata* aqueous extract. *Spectrochim. Acta. A, Mol. Biomol. Spectrosc.* 118, 349–355. <https://doi.org/10.1016/j.saa.2013.08.114>.
- Shamprasad, B.R., Lotha, R., Nagarajan, S., Sivasubramanian, A., 2022. Metal nanoparticles functionalized with nutraceutical Kaempferitrin from edible *Crotalaria juncea*, exert potent antimicrobial and antibiofilm effects against Methicillin-resistant *Staphylococcus aureus*. *Sci. Rep.* 12 (1), 7061. <https://doi.org/10.1038/s41598-022-11004-2>.
- Subramaniyan, S.B., Megarajan, S., Dharshini, K.S., Veerappan, A., 2021. *Artocarpus integrifolia* seed lectin enhances membrane damage, oxidative stress and biofilm inhibition activity of silver nanoparticles against *Staphylococcus aureus*. *Colloids Surf. A Physicochem. Eng. Asp.* 624, <https://doi.org/10.1016/j.colsurfa.2021.126842> 126842.
- Sugimoto, S., Sato, F., Miyakawa, R., Chiba, A., Onodera, S., Hori, S., Mizunoe, Y., 2018. Broad impact of extracellular DNA on biofilm formation by clinically isolated Methicillin-resistant and -sensitive strains of *Staphylococcus aureus*. *Sci. Rep.* 8 (1), 2254. <https://doi.org/10.1038/s41598-018-20485-z>.
- Valliammai, A., Selvaraj, A., Muthuramalingam, P., Priya, A., Ramesh, M., Pandian, S. K., 2021. Staphyloxanthin inhibitory potential of thymol impairs antioxidant fitness, enhances neutrophil mediated killing and alters membrane fluidity of methicillin resistant *Staphylococcus aureus*. *Biomed. Pharmacother.* 141, <https://doi.org/10.1016/j.biopha.2021.111933> 111933.
- Venkatakrishnan, S., Veerappan, G., Elamparuthi, E., Veerappan, A., 2014. Aerobic synthesis of biocompatible copper nanoparticles: promising antibacterial agent and catalyst for nitroaromatic reduction and C-N cross coupling reaction. *RSC Adv.* 4 (29), 15003–15006. <https://doi.org/10.1039/C4RA01126K>.